



Enantioselective binding of amino acids and amino alcohols by self-assembled chiral basket-shaped receptors

Beatriu Escuder,^{*,†} Alan E. Rowan, Martinus C. Feiters^{*} and Roeland J. M. Nolte

Department of Organic Chemistry, Katholieke Universiteit Nijmegen, Toernooiveld 1, NL-6525 ED Nijmegen, The Netherlands

Received 22 October 2002; revised 25 July 2003; accepted 7 November 2003

Abstract—Amino acid appended diphenylglycoluril-based chiral molecular receptors **2** and **3** have been prepared and their aggregation has been studied in water at various pH's and in chloroform. The binding of several biologically relevant guests with aromatic moieties to these aggregates has been studied with UV–Vis spectroscopy in competition experiments with 4-(4-nitrophenylazo)resorcinol (Magneson) and 2-(4-hydroxyphenylazo)benzoic acid (HABA) as probes. Aggregates of chiral host **2b** showed binding of catecholamines and aromatic amino acids in an aqueous environment, as well as discrimination between amino acid enantiomers, and can be considered a mimic for adrenergic receptors.

© 2003 Elsevier Ltd. All rights reserved.

1. Introduction

The design of synthetic molecular receptors that mimic the natural binding sites for hormones, neurotransmitters, and other essential messengers is a topic of intense research with a special emphasis on their enantioselective recognition. Although there is significant progress toward the understanding of the natural systems, synthesis of model compounds can contribute to this understanding and in addition find applications in drug delivery, catalysis, etc.^{1,2} L-Adrenaline has some important biological functions. It belongs to the family of adrenal medulla hormones that have a large influence on the storage and mobilisation of glycogen and fatty acids and the corresponding metabolic pathways. In addition, it is a neurotransmitter of the adrenergic nervous system and has an effect on α and β receptors. The biosynthetic precursors of adrenaline, the catecholamines, have also very interesting biological properties and are of great therapeutical value. In the recent years a great effort has been made in the X-ray crystallographic characterization and modeling of membrane-bound proteins as well as the design of synthetic model receptors for their binding sites.^{3–5} Schrader described phosphonate containing cyclophanes that bind catecholamines and amino acids in organic solvents such as DMSO or methanol and in water.^{6–12} Other authors have reported several crown ether containing receptors that bind, and in

some cases transport, adrenaline, ephedrine, L-dopa and dopamine in water although with moderately low binding constants.^{13–20} More recently, a copper complex of a pyrazole-containing cryptand that binds dopamine in water with a high binding constant has been reported.^{21,22}

Diphenylglycoluril based clip molecules have been prepared and extensively studied in the Nolte group over the past 10 years. These hosts possess a well defined cavity that allows the binding of different phenolic guests via a combination of several non covalent interactions (H-bonding, π – π stacking, and the cavity effect).²³ The introduction of crown ether chains and alkyl tails to these receptors leads to a new generation of the so-called amphiphilic basket receptors, which are able to bind also alkaline metal ions and ammonium salts, and aggregate in water into well defined nanostructures.^{24,25} Here we describe a new series of amino acid appended diphenylglycoluril based receptors bearing L-lysine and L-2,3-diamino propionic acid residues that bind aromatic amino acids and catecholamines in water at different pH values and, in some cases, recognize them enantioselectively.²⁶ As these receptor molecules have pronounced polar and apolar sides, they are amphiphilic and can be expected to aggregate in both aqueous and organic media.²⁷

2. Results and discussion

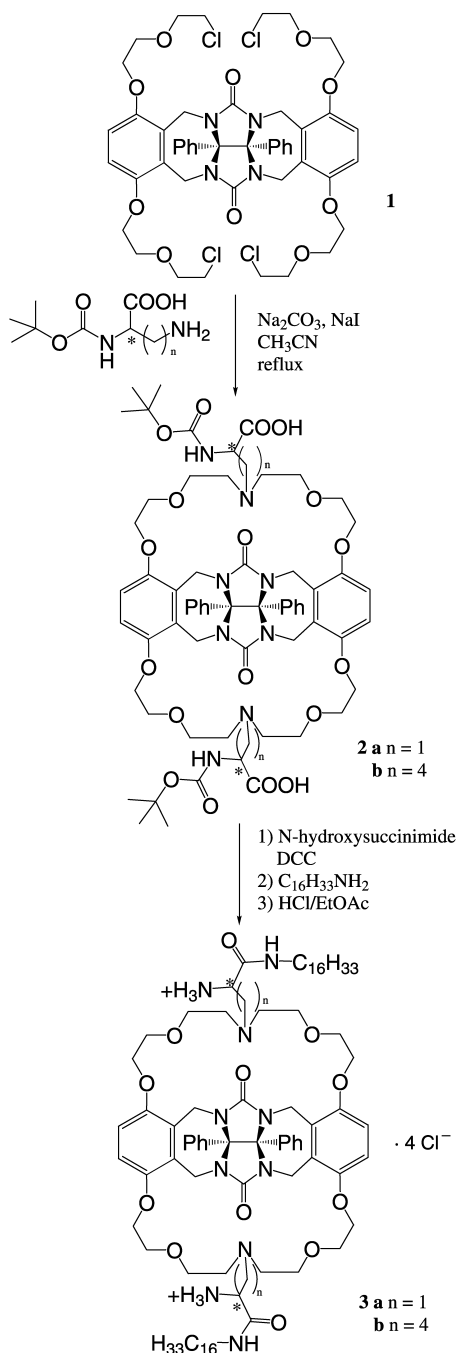
2.1. Synthesis

The synthesis of molecular receptors **2a,b** and **3a,b** was carried out as described in [Scheme 1](#). Compounds **2a,b** were

Keywords: Supramolecular chemistry; Receptors; Enantioselectivity; Amino acids.

* Corresponding authors. Tel.: +34-964-728235; fax: +34-964-728214; e-mail address: escuder@qio.uji.es

† Present address: Dep. Química Inorgànica i Orgànica, Universitat Jaume I, E-12080 Castelló, Spain.



Scheme 1.

prepared in a good yield from the tetrachloride **1** and the corresponding N^{α} -Boc protected amino acid using Finkelstein conditions. The carboxylic acid functions were coupled with two equivalents of hexadecyl amine to give the N -protected precursors of amphiphiles **3a,b**. The t -butoxy-carbonyl protecting group was removed with 4 M HCl in ethyl acetate to give the corresponding hydrochloride as a white precipitate. After slightly basic work-up the free amines were fully characterised by NMR, MS and elemental analysis.

2.2. Aggregation studies

The aggregation behaviour of compounds **2a,b** and **3a,b** was studied in water.²⁸ The critical aggregation concen-

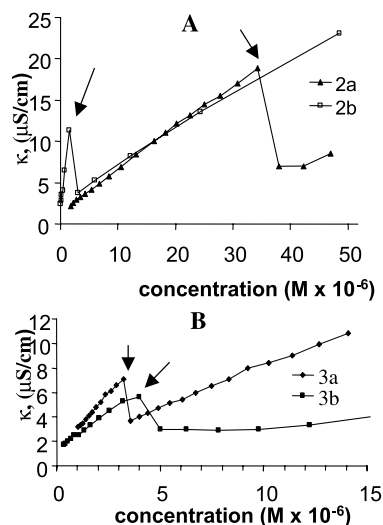


Figure 1. Plot of the conductivity vs concentration of solutions of compounds **2a,b** (A) and (B) **3a,b** in water at 20 °C. (The critical aggregation concentration for each compound is pointed by an arrow. All the experiments were carried out in duplo).

tration (CAC) of these compounds at 20 °C was determined by measuring the conductivity at different concentrations. As can be seen in **Figure 1**, a change in the slope of the plot of the conductivity against the concentration is clearly produced at 3.5×10^{-5} and 1.5×10^{-6} M for **2a** and **2b** respectively, and at 3×10^{-6} and 4×10^{-6} M for **3a** and **3b**. The observed differences are the result of an increase in the mobility of the ions as well as in the number of independent charge carriers upon going from an aggregated towards a non-aggregated state. The difference of one order of magnitude observed between the CAC of compounds **2a** and **2b** is significant enough to be noteworthy. Both compounds exist as zwitterionic species in water but in the case of compound **2a** a six-membered cyclic intramolecular ionic pair could be formed between the carboxylate group and the protonated tertiary nitrogen atom of the aza-crown moiety.

Transmission electron microscopy reveals that receptor **2b** forms vesicles in water with diameters ranging between 50 and 100 nm (**Fig. 2B**). The vesicular structure of the aggregates was confirmed by encapsulation of ethidium bromide. A dispersion of compound **2b** was prepared in the presence of 10^{-4} M ethidium bromide and subsequently filtered through a Sephadex G25 column monitoring the absorbance of **2b** and the fluorescence of the entrapped dye. Fractions containing both compounds were found at elution volumes of ca. 25–100 mL, whereas the free dye was

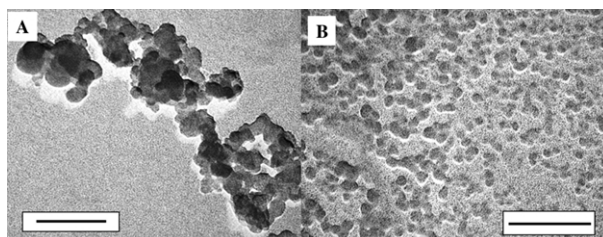


Figure 2. (A) Transmission electron micrograph of a 1% wt dispersion of compound **2a** in water. (B) idem of a dispersion of compound **2b** in water (Pt-shadowing, bars represent 200 nm).

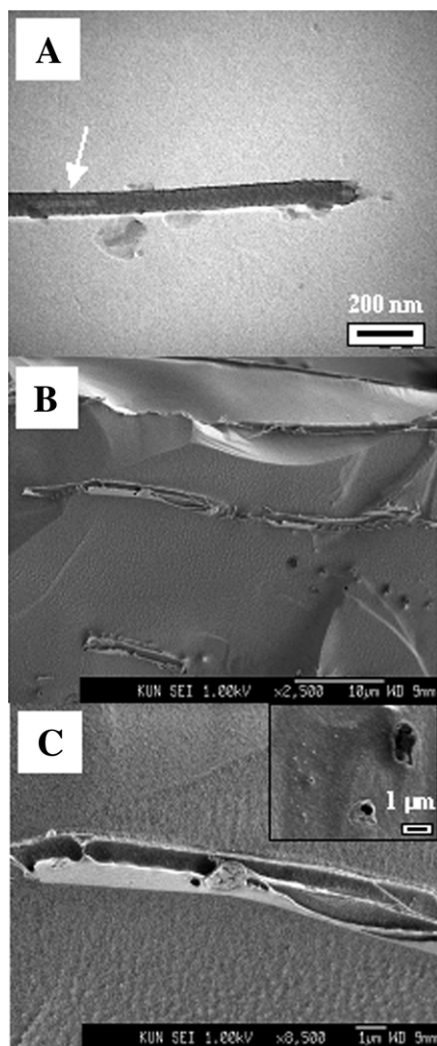


Figure 3. (A) Transmission electron micrographs of a 1% wt dispersion of compound **3a** in water showing tubular architectures (Pt-shadowing). (B) and (C) Cryo-scanning electron micrographs of a 1% wt dispersion of compound **3a** in water showing hollow tubes. The inset shows the side view of the tubes.

retained at the top of the column. In contrast, compound **2a** at the same concentration formed similar but slightly less-defined assemblies in water, only a mixture of round and flat lamellae could be observed (Fig. 2A).

The effect of pH was studied for compound **2b** by transmission electron microscopy (not shown). The dispersion was prepared in 1 mL of 20 mM sodium monophosphate (pH=4.5) and the electron micrographs revealed the presence of the vesicles and their preference for further assembly. The vesicles clustered forming elongated aggregates of various micrometers of length and less than 100 nm width. In contrast to **2b**, compound **3a** aggregates to form thin lamellae in water that roll up to form large tubular objects of several micrometers of length (Fig. 3A). Cryo-SEM micrographs clearly revealed that these tubular objects are in fact hollow tubes of ca. 1 μm diameter and more than 10 μm in length (Fig. 3B).

Transmission electron microscopy of host **3b** in water revealed a mixture of different aggregates (vesicle-like,

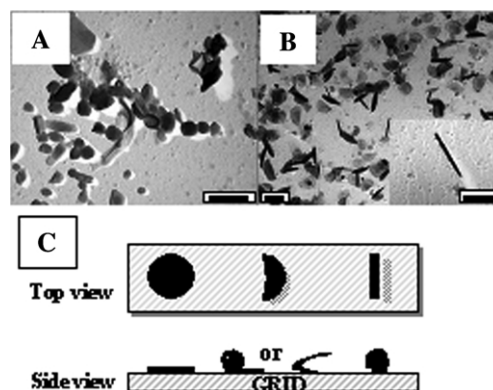


Figure 4. (A) Transmission electron micrographs of a 1% wt dispersion of compound **3b** in water 1 h after sonication. (B) idem after one day. (Pt-shadowing, bars represent 400 nm). (C) Schematic drawing of the aggregates onto the grid.

tubes, flat tapes, see Figure 4A). Upon standing for 1 day, they reorganized to give more uniform lamellar structures. As can be seen in Figure 4B, compound **3b** self-assembles to form flat disks that can fold or roll up to various degrees to give semicircular flat objects and extended structures (Fig. 4C). The same grid was investigated by scanning electron microscopy and it was revealed that flat disk-like objects of ca. 550 nm diameter and 50 nm thickness occur at various angles, along with folded semicircular structures and extended structures which we propose to arise from completely rolled up disks.²⁹ The same aggregates were also observed when the experiment was carried out in 0.1 M HCl (Fig. 5A and B). It is logical to assume that all the amino groups would be protonated in water as well as in the acidic solution. When the assemblies were made in a 0.1 M NaOH aqueous solution, different aggregates were found (Fig. 5C). Flat tapes with lengths between 400 nm and 2.5 μm and widths between 200 and 400 nm were observed together with tubes of 50 nm diameter and similar lengths.

As amphiphiles constructed from lysine and its analogues contain many moieties that can be involved in intermolecular hydrogen bonding, we considered it of interest to also study the aggregation of compounds **2a,b** and **3a,b** in a solvent that would allow the formation of such hydrogen bonds, like chloroform. The strong aggregation of these compounds was already evidenced by the broadening of the ^1H NMR signals in CDCl_3 , in contrast to the sharp resonances observed for solutions of the previously reported *N*-functionalised hosts of this type, and was further confirmed by electron microscopy. Compound **2b** self-assembled into well-defined thin tube-like structures (diameter ca. 5 nm) in chloroform as can be seen in Figure 6A inset. After few hours, these tubular structures further aggregate to give a flat array of aligned and superimposed layers of tubes (Fig. 6A).

In contrast to the previously reported receptors these compounds possess amino acid arms which are the potential sites for additional H-bonding or electrostatic interactions. This feature is thought to be responsible for the observed aggregation behaviour since intermolecular hydrogen bonds can now also be formed between the amide functions leading to extended structures. The aggregation behaviour of molecular receptors **3a** and **3b**, possessing two alkyl tails

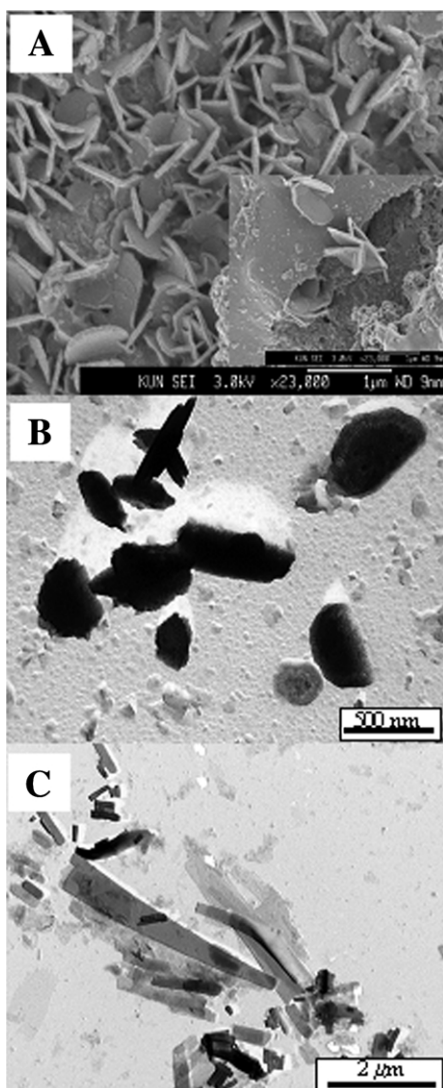


Figure 5. (A) SEM picture of a dispersion of compound **3b** in 0.1 N HCl. (B) Transmission electron micrographs of a dispersion of compound **3b** in 0.1 N HCl (Pt-shadowing). (C) idem in 0.1 N NaOH.

in its structure, was also studied in chloroform by transmission electron microscopy revealing curved bilayer aggregates (Fig. 6B and C).

2.3. Binding studies

The binding of adrenaline and other catecholamines and amino acids by their natural receptors is thought to occur via a combination of non-covalent interactions (viz. electrostatic interactions between aspartate or glutamate protein residues and the ammonium groups of the substrates, H-bonding between the substrate and serine or lysine residues, π - π interactions between the substrate aromatic moiety and the aromatic residues of the protein, and the π -cation interaction between the ammonium group and the electron-rich aromatic system of tyrosine and tryptophan residues).⁵ On the other hand, an important goal for the design of synthetic receptors is the enantioselective recognition of guests. Considerable work has been devoted to the design and syntheses of chiral hosts for amino acids and other biologically relevant guests.^{30–39} Compounds

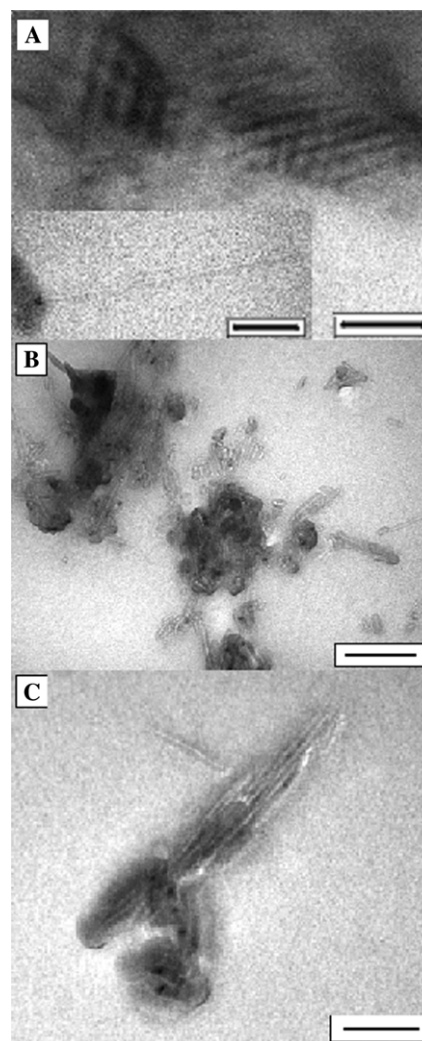


Figure 6. Transmission electron micrographs of 1% wt. CHCl_3 solutions of (A) compound **2b**, (B) compound **3b** and (C) compound **3a**. (Pt-shadowing, bars represent 100 nm).

2a,b possess the chiral functionalities required to perform such enantioselectivity. The hosts present a pocket-like geometry and also their aggregation behaviour suggests that they could be incorporated easily into a membrane as a carrier or membrane-bound receptor mimic.

UV–Vis spectroscopy was used for the determination of the binding constants. The absorption signals of both the host and the guest unfortunately overlapped and here a competition experiment was carried out using Magneson (**4**, 4-(4-nitrophenylazo)resorcinol) or HABA (**5**, 2-(4-hydroxyphenylazo)benzoic acid) as a competing dye (Chart 1). The binding of Magneson by compound **2b** was studied in water at 20 °C by UV–Vis spectroscopy above its CAC.⁴⁰ When a sample containing the dye (**4**) was titrated with **2b** an increase in the absorbance at 450 nm was observed reaching almost complete saturation when ca. 2 equiv. of the host molecule were added. It was recently shown that for similar host molecules, this behaviour is in accordance with the formation of vesicles in which only half of the sites are available for binding the guest.²⁵ The addition of excess host induced small changes in the UV spectra probably because the vesicle bilayer is not a

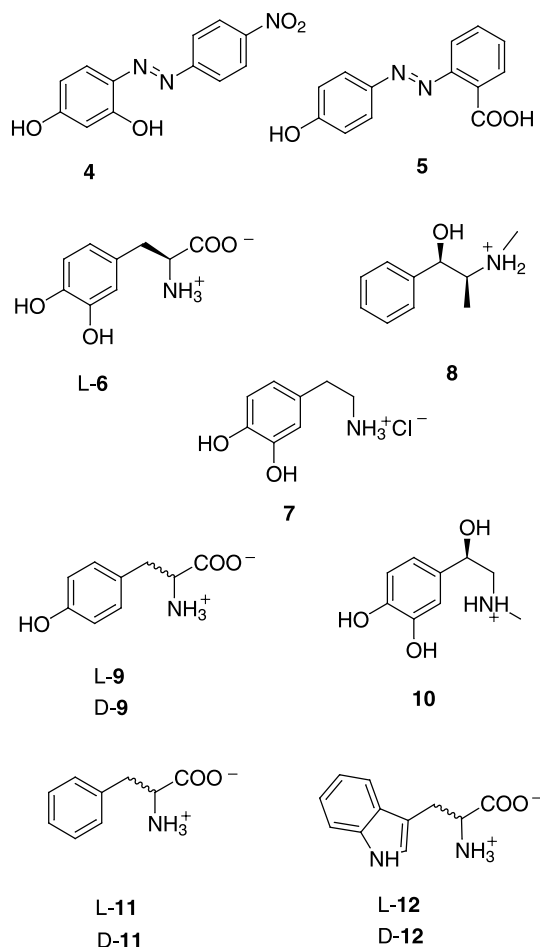


Chart 1.

sufficiently impermeable barrier and some molecules of Magneson (**4**) can cross it and be bound by the inner binding sites. The binding constant for Magneson (**4**) was calculated by fitting the data assuming only half of the hosts bound in a 1:1 host–guest ratio, $K_{\text{ass}} = (4.4 \pm 1.2) \times 10^4 \text{ M}^{-1}$ (Table 1).

The binding of the different guests (Chart 1) with compound **2b** was first studied above its CAC at pH=8 by UV–Vis competition by adding different amounts of the guest to a solution containing the host **2b** and Magneson (**4**).⁴¹ The Magneson absorption band at 450 nm decreases with the addition of the guest and the presence of an isosbestic point at ca. 290 nm agrees with the presence of a single complexation equilibrium which can be fitted to a 1:1 complex stoichiometry.

Table 1. Binding parameters of compound **2b** with the probes **4** and **5** at 20 °C

Probe	Solvent	$K_{\text{ass}} (\text{M}^{-1})^{\text{a,b}}$	$\Delta \epsilon^{\text{b,c}}$	$\Delta G (\text{kJ mol}^{-1})^{\text{b}}$
4	pH 8 buffer ^d	$(4.4 \pm 1.2) \times 10^4$	17,150	-26.0(0.7)
5	pH 4.5 buffer ^d	$(2.5 \pm 0.2) \times 10^4$	3724	-24.7(0.2)

^a All the experiments were carried out in duplo.

^b Errors are given between parentheses.

^c Difference between the extinction coefficients of guest and complex in absolute value.

^d 0.02 M phosphate buffer solutions.

Table 2. Estimated binding parameters for **2b** and guests **6–12** determined by UV–Vis competition with Magneson **4** and HABA **5** at 20 °C

Probe	Guest	$K_{\text{ass}} (\times 10^3 \text{ M}^{-1})^{\text{a}}$	$\Delta G (\text{kJ mol}^{-1})^{\text{a}}$	$\Delta \Delta G (\text{kJ mol}^{-1})^{\text{b}}$
4 ^c	6	4(1)	-20.2(0.6)	—
4 ^c	7	0.9(0.5)	-16.5(1.3)	—
4 ^c	8	4.7(0.4)	-20.6(0.2)	—
4 ^c	L- 9	10(3)	-22.4(0.7)	—
5 ^d	6	1.9(0.3)	-18.4(0.4)	—
5 ^d	7	1.7(0.4)	-18.1(0.6)	—
5 ^d	8	4.7(0.5)	-20.6(0.3)	—
5 ^d	L- 9	2.2(0.5)	-18.7(0.6)	4.9
5 ^d	D- 9	16(2)	-23.6(0.3)	—
5 ^d	10	12.8(0.5)	-23.0(0.1)	—
5 ^d	L- 11	26(5)	-24.7(0.5)	-1.8
5 ^d	D- 11	12(1)	-22.9(0.2)	—
5 ^d	L- 12	17(2)	-23.7(0.3)	2.9
5 ^d	D- 12	56(7)	-26.6(0.3)	—

^a Errors given between parentheses.

^b Value for the difference $\Delta G_{\text{L}} - \Delta G_{\text{D}}$.

^c Magneson (**4**), pH 8, 450 nm.

^d HABA (**5**), pH 4.5, 350 nm.

For guests **6–9** moderate values for the binding constant were found (Table 2). Upon comparison of the relative guest structures the differences in K_{ass} can be attributed to either the presence or absence of the hydroxyl functions in the aromatic ring and the carboxylate group in the side chain. The highest binding constant was observed for L-tyrosine (L-**9**), $K_{\text{ass}} = (10 \pm 3) \times 10^3 \text{ M}^{-1}$. This value slightly decreases when either the phenolic group is not present as in the case of ephedrine (**8**), $K_{\text{ass}} = (4.7 \pm 0.4) \times 10^3 \text{ M}^{-1}$, or when an extra hydroxyl is introduced, as in L-dopa (L-**6**), $K_{\text{ass}} = (4 \pm 1) \times 10^3 \text{ M}^{-1}$. The effect of repulsion of a negative charge in the guest by the negatively charged carboxylates in the host is noticeable in the in K_{ass} going from dopamine (**7**), which lacks the carboxylate, to L-dopa (**6**), where it is present. As is well known, one of the main forces responsible for the binding of guests in hosts in water is the hydrophobic interaction. The release of water molecules from the cavity when the guest is bound and the decrease of the apolar surface in contact with water in the complex both favour binding. This will be a common factor for all the guests that we studied. All of them possess a hydrophobic aromatic moiety by which the molecule is pulled into the

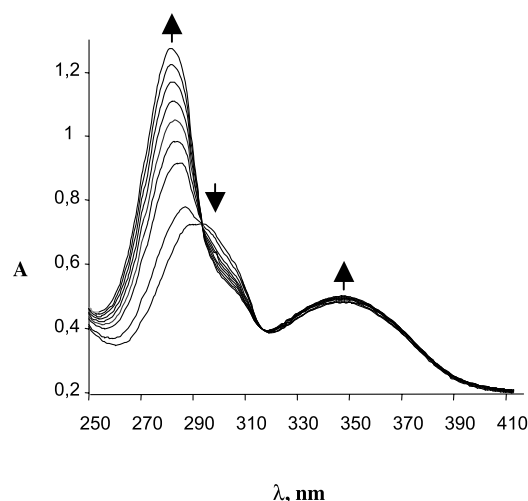


Figure 7. UV/VIS binding competition curves for the **2b**:2-(4-hydroxyphenylazo)benzoic acid (**5**) complex with L-dopa (**6**) at pH=4.5.

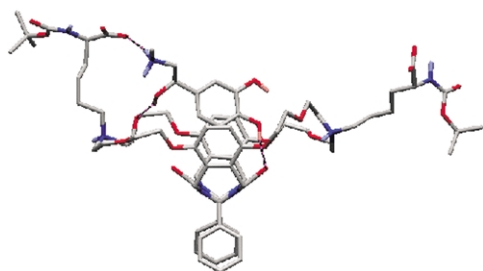


Figure 8. Calculated minimum energy geometry for the 1:1 complex of **2b** and adrenaline (**10**), hydrogen atoms have been omitted for clarity.

cavity while the differences in binding between them are caused by differences in solvation and the differing complementarity between the guests and the host. Thus, an increase in the number of hydroxyl functions will, in principle, increase the solvation of the guest in water and then decrease slightly the binding constant as is obvious from a comparison of the binding constants of dopamine (**7**) with ephedrine (**8**). The later which lacks OH groups would be more poorly solvated by water and then bound deeper in the cavity. Although it is a more polar group, the presence of a carboxylate also exerts a favourable effect, either by orientating the guest inside the cavity or by electrostatic charge–charge or dipole–charge interactions.

The important role that π -cation interactions play in biological binding sites is well documented.^{42,43} The protonated nitrogen atoms on the aza-crown moiety could play a role in the binding process. In order to ensure the full protonation of the tertiary amino functions of the azacrown moieties the binding studies were also carried out at slightly acidic conditions in a 0.02 M NaH_2PO_4 buffer solution of pH 4.5.⁴⁴ For these studies, HABA (2-(4-hydroxyphenyl-azo)benzoic acid, **5**), with a binding constant of $(2.5 \pm 0.2) \times 10^4 \text{ M}^{-1}$ for the 1:1 complex with **2b**, was used as a UV–Vis probe instead of Magneson (**4**), because the later had inconvenient additional absorption bands at low pH. Following a similar procedure as for the former

case the binding of guests **6–12** with host **2b** was studied (Table 2). The absorption spectra for the competition experiments with HABA (**5**) and L-dopa (**6**) in host **2b** are shown in Figure 7. In this case, the absorption band of HABA at ca. 350 nm increases upon the addition of the guest.

The binding constants for host **2b** with L-dopa (L-**6**), dopamine (**7**) and ephedrine (**8**) measured at pH 4.5 were similar to those observed at higher pH. In contrast to binding at pH 8, the binding of L-tyrosine (L-**9**) is reduced at pH 4.5 (Table 2). The binding of adrenaline (**10**) as a guest was also studied giving a binding constant of $(12.8 \pm 0.5) \times 10^3 \text{ M}^{-1}$, one order of magnitude larger than those obtained for the former guests, and considerably higher than the values found in literature in aqueous solution.^{10,16} In this case, the presence of the methyl group increases the hydrophobicity of the guest resulting in a strong binding spite of the presence of OH groups in the molecule. In order to prove the role played by the carboxylate groups in the binding of this kind of guests both enantiomers of the amino acids phenylalanine (L-**11**, D-**11**) and tryptophan (L-**12**, D-**12**) as well as the D-tyrosine (D-**9**) were also studied. In all cases, the binding constants were one order of magnitude higher than those obtained for dopamine (**7**) and ephedrine (**8**). It is clear that electrostatic or charge–dipole interactions play an important role in the binding process.

2.4. Enantioselective binding

Enantioselective binding was observed when the pair of enantiomers of tyrosine (L-**9**, D-**9**), phenylalanine (L-**11**, D-**11**) and tryptophan (L-**12**, D-**12**) were studied (see Table 2). In the first case, a $\Delta\Delta G$ ($\Delta G_L - \Delta G_D$) of 4.9 kJ/mol was found in favour of the D-enantiomer (D-**9**). In a racemic guest solution almost 90% of the binding sites would be occupied by the D-enantiomer. For the pair of enantiomers of phenylalanine (L-**11**, D-**11**) there is 1.8 kJ/mol more loss of free energy for the binding of the L-enantiomer (L-**11**) and in the case of tryptophan (L-**12**, D-**12**) the difference was of

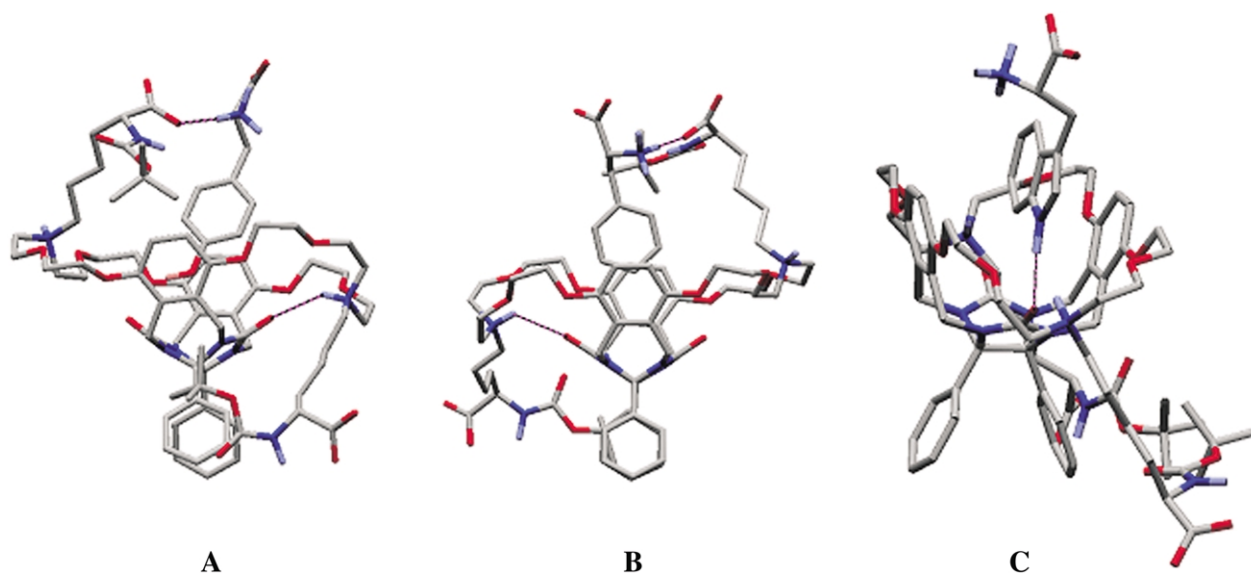


Figure 9. Calculated minimum energy complexation geometries for the 1:1 complexes of **2b** and (A) D-tyrosine (D-**9**), (B) L-phenylalanine (L-**11**) and (C) D-tryptophan (D-**12**), hydrogen atoms have been omitted for clarity.

2.9 kJ/mol in favour of the D-enantiomer (D-**12**). Although the enantioselectivities observed are moderate they are significant. The binding geometries for the three pairs of enantiomers at first glance seem to be quite similar and independent of the different aromatic moieties they present. The reverse enantioselectivity of the complex with **11** as compared to **9** and **12**, which contain a phenolic hydroxy group and an indole nitrogen, respectively, must be due to H-bonding interactions inside the cavity, as confirmed by our modelling studies (see Section 2.5).

2.5. Modelling studies⁴⁵

Computational studies have been widely used in the last years for the modelling of chiral recognition systems such as cyclodextrins, proteins and synthetic receptors.^{46–50} Here we used a Monte Carlo/Molecular dynamics mixed approach for an approximation of the structure of the host–guest complexes coherent with the experimental results (see Section 4 for details). In most cases, the minimum energy conformers found showed the guest placed inside the cavity. For the same host–guest complex, the main difference between the calculated energy of the collected structures was in the Van der Waals and solvation terms, in agreement with the hydrophobic effect being the driving force of the inclusion process. In fact, the minimum energy conformations always showed the smallest molecular surface area exposed to the solvent. On the other hand, the largest favourable energetic term seems to correspond to the electrostatic interactions. This could explain the higher binding observed when the guest contained a carboxylate group in its structure as in tyrosine (**9**), phenylalanine (**11**), and tryptophan (**12**) compared with dopamine (**7**) and ephedrine (**8**).

In general, the lowest energy conformations of the complexes between **2b** and the different guests always showed the guest bound inside the cavity. As an example, Figure 8 shows the calculated structure for the complex between adrenaline (**10**) and **2b**. It can be seen that the binding again involves electrostatic interactions, this time between the ammonium group of the guest and one of the carboxylates of the host, in addition to the extra hydrophobicity provided by the methyl group, as mentioned earlier (cf. previous section) as well as H-bonding and aromatic hydrophobic interactions. The complex structures found for the guests **9**, **11** and **12** are also in agreement with the enantioselectivity observed in the experimental binding studies (Fig. 9). For the complex between **2b** and D-tyrosine (D-**9**) all the minimum energy conformers have the guest placed inside the cavity. The main difference between the different minima is the possibility of H-bonding between the phenolic OH of the guest and the C=O of the uril moieties. In the case of the binding of the enantiomer L-tyrosine (L-**9**) the conformations found for its complex with **2b** showed a more flexible geometry. Thus, the guest L-**9** appeared in different dispositions inside the cavity and bound by the lysine arms in a smaller energy range of less than 20 kJ/mol. Nevertheless, a clear energetic preference was calculated for those complexes with the guest located inside the cavity, and no structures were found with the guest outside the cavity. Even more clear results were calculated in the case of tryptophan (**12**) guests. The D-enantiomer (D-**12**) fits into

the cavity and seems to be clipped-on by a H-bond between the indole NH group and the carbonylic oxygen from the uril moiety whereas L-tryptophan (L-**12**) is more flexible. The distance between the uril carbonylic oxygen and the indole NH of tryptophan as well as the phenolic OH of the tyrosine was monitored during the Molecular Dynamics simulation. As can be seen in Figure 10C, the 80% of the population showed an average distance in the range of 1.5–3.5 Å in the case of D-**12** and no conformation in a distance above 7 Å was found, whereas for the diastereomeric complex L-**12** the 70% of the population was found within this average distance, 25% between 3.6 and 7 Å and 5% above 7 Å. The majority of the conformers show for both enantiomers distances below 4 Å and agrees with the guest being confined into the cavity, the presence of conformations with larger distances in the L-enantiomer being related to the larger looseness of the complex. In the case of

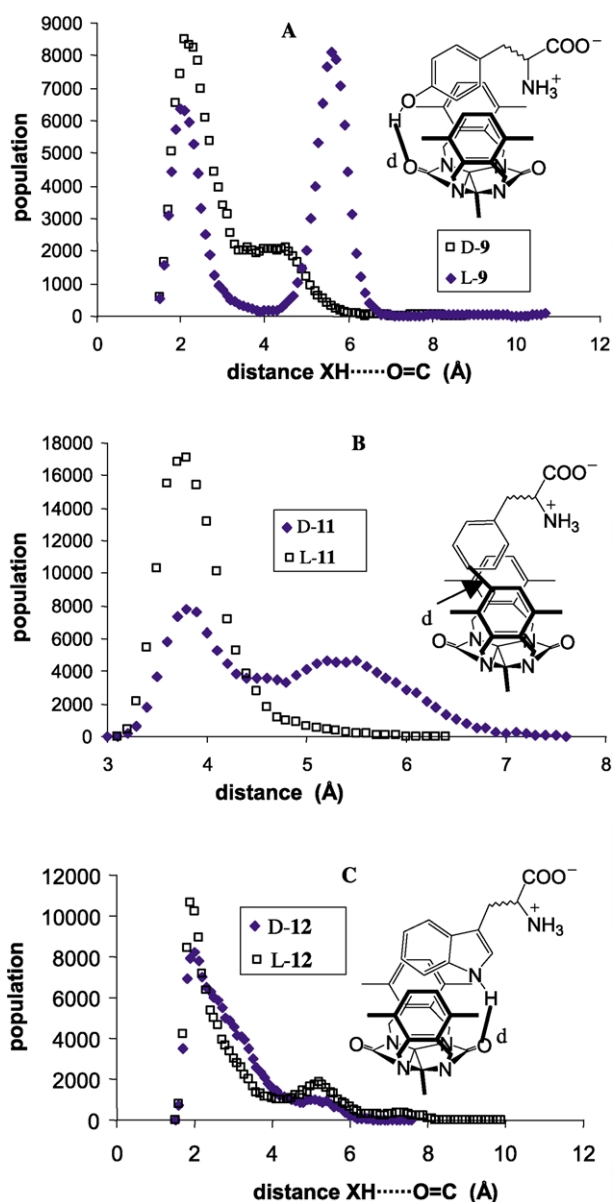


Figure 10. Distribution of complexation geometries (133,333 structures) during 2000 ps of molecular dynamics simulation vs the selected host–guest distances for **2b** and (A) tyrosine (**9**), (B) phenylalanine (**11**) and (C) tryptophan (**12**).

tyrosine, there is a clear difference between the observed behaviour of the two complexes (Fig. 10A). Whereas the complex with D-9 shows a major population of conformers between 1.6 and 3.5 Å the diastereomeric complex with L-9 presents two clearly different populations, the first at 2–3 Å and the second at 5–7 Å. In this case the guest D-9 is much better accommodated into the cavity than the guest L-9. In the case of phenylalanine (11), the conformational population also points to a more defined complex with the experimentally preferred enantiomer, L-11 (Fig. 10B).

3. Conclusions

We have presented a new series of diphenylglycoluril-based amino acid-tethered cavity containing receptors with remarkably versatile aggregation behaviour in both water and chloroform solutions. In particular, compound 2b forms thin tubules in chloroform, whereas it forms vesicles in water. The long tail derivatives 3a,b form large aggregates that can also be tuned with the pH of the medium. Compounds 2a,b present a variety of interaction sites that allow the strong binding of biologically relevant molecules such as amino acids and catecholamines via a combination of several non-covalent interactions. In general, the binding constants calculated for 2b with these guests are moderate to high and a remarkable enantioselectivity for D-tyrosine (D-9), L-phenylalanine (L-11) and D-tryptophan (D-12) with respect to their antipodes is shown at pH 4.5. The aggregation and binding features described here will be exploited in the future with the incorporation of these receptors into membranes for their study as cell-surface adrenergic receptor mimics, as well as their potential use in drug delivery or catalysis.

4. Experimental

4.1. General remarks

NMR spectra were recorded on a Bruker AC-300 (¹H NMR 300 MHz) and Bruker FAMX500 (¹H NMR 500 MHz) spectrometers in CDCl₃ with TMS as internal standard. UV–Vis spectra were recorded with a Varian Cary 50Conc spectrophotometer. Compound 1 was prepared as reported before⁵¹ and the *N*^α-Boc protected amino acids were obtained from FLUKA. Magneson (4) and HABA (5) were purchased from Aldrich.

4.1.1. Molecular receptor 2(a,b). A mixture of compound 1 (4.05 mmol), NaI (40 g, 0.27 mol) and Na₂CO₃ (13.3 g, 0.13 mol) in 500 mL of acetonitrile was refluxed under nitrogen for 4 h. The *N*^α-Boc-protected amino acid (12.2 mmol) was then added in small portions over a period of 2 days and the mixture was refluxed for one week. After filtration and evaporation of the solvent the crude white solid was suspended in CHCl₃ and washed with 10% citric acid and water. The organic layer was dried (Na₂SO₄) and concentrated under vacuum. After column chromatography (neutral alumina, eluent 0.1–0.5% MeOH/CHCl₃, v/v) pure 2(a,b) was obtained as a solid. 2a (87%). Mp 180 °C dec. [α]_D²⁰ = +8.72° (*c* = 1, CHCl₃). ¹H NMR (CDCl₃/CD₃OD, 8/2): 1.3 (m, 18H); 2.5–2.8 (m, 6H); 3.5–4.1 (m, 36H); 5.4

(m, 4H); 6.7 (m, 4H); 7.0 (s, 10H). ESI-MS *m/z* = 626.5 [M+2H]²⁺. Anal. Calcd for C₆₄H₈₂N₃O₁₈: C. 61.43; H. 6.60; N. 8.95. Found: C. 61.01; H. 6.82; N. 8.64. 2b (62%). Mp 128 °C. [α]_D²⁰ = +5.85° (*c* = 0.65, CHCl₃). ¹H NMR (CDCl₃): 1.2–2.0 (m+s, broad, 32H); 2.3–3.0 (m, 12H); 3.5–4.6 (m, 30H); 5.5 (m, 4H); 6.71 (m, 4H); 7.10 (s, broad, 10H). FAB-MS *m/z* = 1335.8 [M+H]⁺. Anal. Calcd for C₇₀H₉₄N₈O₁₈: C. 62.95; H. 7.09; N. 8.39. Found: C. 62.71; H. 6.78; N. 8.17.

4.1.2. Amphiphilic receptor 3 (a,b). Compound 2(a,b) (0.34 mmol) and *N*-hydroxysuccinimide (0.69 mmol) were dissolved in dry dimethoxy ethane and cooled at 0 °C. Then DCC was added and the mixture was kept in the refrigerator for 24 h. Afterwards, the white precipitate was filtered off and to the resulting solution hexadecylamine (0.69 mmol) was added at 0 °C. The reaction was stirred overnight at room temperature and the white solid formed was filtered-off and washed with a small amount of diethyl ether. Finally, the solid was suspended in a 4 M HCl solution in ethyl acetate and after stirring at room temperature during 2 h compound 3(a,b) precipitated as the hydrochloride. Further slightly basic work-up lead to the free amines. 3a: (63%). Mp 235 °C dec. [α]_D²⁰ = –6.11° (*c* = 0.4, CH₃OH). ¹H NMR (CDCl₃): 0.87 (t, 6H); 1.2–1.4 (s+m, 56H); 2.5–3.3 (m, 6H); 3.5–4.3 (m, 40H); 5.6 (m, 4H); 6.7 (m, 4H); 7.1 (s, 10H). ESI-MS *m/z* = 896.5 [M–2(C₁₆H₃₃NHCOCH₂[–]) + Na]⁺. Anal. Calcd for C₈₆H₁₃₂N₁₀O₁₂: C. 69.84; H. 8.88; N. 9.35. Found: C. 69.71; H. 9.08; N. 9.11. 3b: (58%). Mp 250 °C dec. [α]_D²⁰ = +3.04° (*c* = 0.23, CH₃OH). ¹H NMR (CDCl₃): 0.87 (t, 6H); 1.24 (s broad, 52H); 1.5–2.2 (m broad, 16H); 3.2–4.2 (m broad, 42H); 5.6 (m, 4H); 6.7 (m, 4H); 7.1 (s, 10H). FAB-MS *m/z* = 1583.2 [M+H]⁺. Anal. Calcd for C₉₂H₁₄₄N₁₀O₁₂: C. 69.84; H. 9.17; N. 8.85. Found: C. 69.51; H. 9.42; N. 8.44.

4.2. Electron microscopy

Aggregates preparation. The compounds were dissolved in ca. 50 mL of methanol, injected into the aqueous solution at room temperature to a final concentration of 0.1–1 mg/mL and sonicated at 40 °C for 30 min. Different samples were studied between two hours and few days after sonication. Chloroform samples were made by dissolving 1 mg or less of the compound in 1 mL of the solvent.

Transmission electron microscopy. TEM was carried out with a JEOL JEM.1010 electron microscope. The aqueous samples were prepared by adding a drop of the solution over a copper grid covered with a thin layer of formvar. After a few seconds (depending on the concentration of the sample and its affinity for the polymer surface) the sample was drained and left to dry at room temperature overnight. When chloroform was used as a solvent, the samples were prepared in a similar way but over a hydrophobic carbon coated copper grid. Before observation, the samples were shadowed with Pt at 45°.

Scanning electron microscopy. The samples were studied with a Field Emission Scanning Electron Microscope Jeol JSM-6330F. They were prepared in a similar way as before on a copper grid covered with a thin layer of formvar and then they were sputtered with 1.5 nm of Au/Pd.

Cryo-scanning electron microscopy. The samples were studied with a Field Emission Scanning Electron Microscope Jeol JSM-6330F. A drop of the sample solution was placed in a stub and it was quickly cooled down at $-220\text{ }^{\circ}\text{C}$ with under-cooled nitrogen as slush. The sample was then introduced into the microscope cooling pre-chamber and it was allowed to warm up until $-95\text{ }^{\circ}\text{C}$. At this temperature the upper part of the drop was fractured with a cool knife and etched for 2 min. Then, the pre-chamber was cooled down until $-120\text{ }^{\circ}\text{C}$ and the sample was sputtered in situ with 1.5 nm of Au/Pd. Finally, it was transferred into the microscope chamber where the temperature was kept below $-130\text{ }^{\circ}\text{C}$ to avoid the formation of ice crystals.

4.3. Conductivity measurements

Conductivity measurements were performed in duplo with a Schott Geräte CG 852 Conductimeter with a platinum electrode at room temperature. Stock solutions of the receptors were diluted several times until very low concentrations were achieved while continuously monitoring the conductivity.

4.4. Encapsulation of ethyidium bromide

The encapsulation of ethyidium bromide was measured by gel permeation chromatography (GPC) in combination with fluorescence and UV–Vis spectroscopy. The desired vesicular dispersion was prepared in water containing 10^{-4} M ethyidium bromide and passed over a Sephadex G25 column with water as eluent. The fluorescence intensity of ethyidium bromide ($\lambda_{\text{ex}}=480\text{ nm}$, $\lambda_{\text{em}}=630\text{ nm}$) as well as the absorbance of the host molecule at 288 nm was monitored.

4.5. UV binding studies

All the experiments were carried out using double distilled water or freshly distilled chloroform to prepare the solutions. In a typical experiment a conveniently buffered solution of the dye (ca. $2\times 10^{-5}\text{ M}$) was titrated by adding small amounts of a solution containing the host and the dye (ca. $2\times 10^{-5}\text{ M}$). The change in the absorbance (450 nm for Magneson (**4**) and 350 nm for HABA (**5**)) was plotted against the total host concentration. The data were fitted using Eq. 1 with an Excel spreadsheet.

$$[\text{HG}]_i = 0.5((H_t + G_t + 1/K_{\text{ass}}) - \sqrt{(H_t + G_t + 1/K_{\text{ass}})^2 - (4H_tG_t)}) \quad (1)$$

The fitting was compared with the double-reciprocal plot graphical method,^{52,53} giving a linear plot for the data, corresponding to the first 0.5 equiv. of guest in the case of Magneson, in agreement with the values estimated before with non-linear fitting of expression 1.

In a typical competition experiment, an appropriate buffer solution containing the host and the probe in ca. 3×10^{-5} and $1.6\times 10^{-5}\text{ M}$ concentration, respectively, was titrated with a guest solution which was also $1.6\times 10^{-5}\text{ M}$ in the probe. The binding constant for each guest was calculated at several total guest concentrations, always in the range of 20 to 80%

of complexation, using the following equations in an Excel spreadsheet

$$A_i = \varepsilon_{\text{D}}[\text{D}]_i + \varepsilon_{\text{DH}}[\text{HD}]_i = \varepsilon_{\text{D}}D_t + (\varepsilon_{\text{DH}} - \varepsilon_{\text{D}})[\text{HD}]_i \quad (2)$$

$$[\text{HD}]_i = \frac{A_i - \varepsilon_{\text{D}}D_t}{\varepsilon_{\text{DH}} - \varepsilon_{\text{D}}} \quad (3)$$

$$[\text{D}]_i = D_t - [\text{HD}]_i \quad (4)$$

$$[\text{H}]_i = \frac{[\text{HD}]_i}{K_{\text{D}}[\text{D}]_i} \quad (5)$$

$$K_{\text{G}} = \frac{[\text{HG}]_i}{[\text{H}]_i[\text{G}]_i} = \frac{H_t - [\text{H}]_i - [\text{HD}]_i}{[\text{H}]_i(G_t - (H_t - [\text{H}]_i - [\text{HD}]_i))} \quad (6)$$

where A_i is the absorbance at the studied wavelength for the experiment i , $[\text{X}]_i$ the concentration of the host (H), guest (G), dye (D), host–probe complex (HD) and host–guest complex (HG) for the experiment i , X_t the total concentration of host (H), guest (G) and dye (D) in the experiment i , K_{D} the known binding constant of the probe (D), and K_{G} is the calculated binding constant for the guest G.

The binding constant values estimated were finally averaged and the standard deviations calculated. The extinction coefficients were calculated in separate experiments and blank experiments were carried out to check possible interferences of the guest on the absorption band of the dye in the absence of host.

4.6. Modelling studies

Molecular mechanics docking calculations were performed for the complex structures using the Monte Carlo conformational search method implemented in the MacroModel V7.0 program.⁵⁴ The AMBER* force field was used in a water continuous solvent simulation (GB/SA).⁵⁵ Energy minima were found and the conformational space close to them was explored by performing molecular dynamics simulations. Starting structures were drawn with different disposition of the guest inside and outside the cavity of the host. In each case, the conformational search was performed with 3000 iterations for each step and structures were collected in a 50 kJ/mol energy window. Then, molecular dynamics simulations were performed on the energy minima obtained with a total simulation time of 2000 ps.

Acknowledgements

The authors thank H. P. M. Geurts for technical support in the electron microscopy studies. B.E. also thanks the European Community for a postdoctoral Marie Curie TMR grant.

References and notes

1. *Supramolecular Reactivity and Transport: Bioorganic Systems. Comprehensive Supramolecular Chemistry*; Murakami, Y., Ed.; Elsevier: Amsterdam, 1996; Vol. 3. Lehn, J.-M., ed.; Atwood, J. L.; Davies, J. E. D.; Macnicol, D. D.; Vögtle, F. executive eds.
2. (a) Kikuchi, J. I.; Murakami, Y. *J. Incl. Phen. Mol. Rec. Chem.*

- 1998, 32, 209–221. (b) Kikuchi, J. I.; Ariga, K.; Ikeda, K. *Chem. Commun.* **1999**, 547–548.
3. Stryer, L. *Biochemistry*. 3rd ed. W. H. Freeman: New York, 1988.
4. Silverman, R. B. *The Organic Chemistry of Drug Design and Drug Action*; Academic: New York, 1992.
5. Trumpp-Kallmeyer, S.; Hoflack, J.; Bruinvels, A.; Hilbert, M. *J. Med. Chem.* **1992**, 35, 3448–3462.
6. Schrader, T. *Angew. Chem. Int. Ed. Engl.* **1996**, 35, 2649–2651.
7. Schrader, T. *J. Org. Chem.* **1998**, 63, 264–272.
8. *Bioorganic Chemistry. Highlights and New Aspects*; Diederichsen, U., Lindhorst, T. K., Westermann, B., Wessjohann, L. A., Eds.; Wiley-VCH: Weinheim, 1999; p 215.
9. Herm, M.; Schrader, T. *Chem. Eur. J.* **2000**, 6, 47–53.
10. Herm, M.; Molt, O.; Schrader, T. *Angew. Chem. Int. Ed.* **2001**, 40, 3148–3151.
11. Grawe, T.; Schrader, T.; Finocchiaro, P.; Consiglio, G.; Failla, S. *Org. Lett.* **2001**, 3, 1597–1600.
12. Rensing, S.; Arendt, M.; Springer, A.; Grawe, T.; Schrader, T. *J. Org. Chem.* **2001**, 66, 5314–5821.
13. Behr, J. P.; Lehn, J. M.; Vierling, P. *Helv. Chim. Acta* **1982**, 65, 1853–1867.
14. Kimura, E.; Fujioka, H.; Kodama, M. *J. Chem. Soc., Chem. Commun.* **1986**, 1158–1159.
15. Hayakawa, K.; Kido, K.; Kanematsu, K. *J. Chem. Soc., Perkin Trans. 1* **1988**, 511–519.
16. Bernardo, A. R.; Stoddart, J. F.; Kaifer, A. E. *J. Am. Chem. Soc.* **1992**, 114, 10624–10631.
17. Ishizu, T.; Hirayama, J.; Noguchi, S. *Chem. Pharm. Bull.* **1994**, 42, 1146–1148.
18. Paugam, M. F.; Valencia, L. S.; Boggess, B.; Smith, B. D. *J. Am. Chem. Soc.* **1994**, 116, 11203–11204.
19. Paugam, M. F.; Bien, J. T.; Smith, B. D.; Christoffels, L. A. J.; de Jong, F.; Reinhoudt, D. H. *J. Am. Chem. Soc.* **1996**, 118, 9820–9825.
20. Campayo, L.; Bueno, J. M.; Navarro, P.; Ochoa, C.; Jiménez-Barbero, J.; Pèpe, G.; Samat, A. *J. Org. Chem.* **1997**, 62, 2684–2693.
21. Lamarque, L.; Miranda, C.; Navarro, P.; Escartí, F.; García-España, E.; Latorre, J.; Ramírez, J. A. *Chem. Commun.* **2000**, 1337–1338.
22. Lamarque, L.; Navarro, P.; Miranda, C.; Arán, V. J.; Ochoa, C.; Escartí, F.; García-España, E.; Latorre, J.; Luis, S. V.; Miravet, J. F. *J. Am. Chem. Soc.* **2001**, 123, 10560–10570.
23. Rowan, A. E.; Elemans, J. A. A. W.; Nolte, R. J. M. *Acc. Chem. Res.* **1999**, 32, 995–1006.
24. Schenning, A. P. H. J.; de Bruin, B.; Feiters, M. C.; Nolte, R. J. M. *Angew. Chem. Int. Ed.* **1994**, 33, 1662–1663.
25. Schenning, A. P. H. J.; Escuder, B.; van Nunen, J. L. M.; de Bruin, B.; Löwik, D. W. P. M.; Rowan, A. E.; Van der Gaast, S. J.; Feiters, M. C.; Nolte, R. J. M. *J. Org. Chem.* **2001**, 66, 1538–1547.
26. For earlier reports on lysine based amphiphiles see: Reichel, F.; Roelofsen, A. M.; Geurts, H. P. M.; van der Gaast, S. J.; Feiters, M. C.; Boons, G. J. *J. Org. Chem.* **2000**, 65, 3357–3366. Zarif, L.; Gulik-Krzwycki, T.; Riess, J. G.; Pucci, B.; Guedj, C.; Pavia, A. A. *Colloids Surf. A* **1994**, 84, 107–112.
27. Part of this work has been published as a communication: Escuder, B.; Rowan, B.; Feiters, A. E.; Nolte, M. C. *Tetrahedron Lett.* **2001**, 42, 2751–2753.
28. The pH values measured upon dispersion in unbuffered water are as follows: **2a**, pH=6.5; **2b**, pH=7.9; **3a**, pH=7.2; **3b**, pH=7.9.
29. This observation can be due to a sample preparation artefact because of a vacuum effect.
30. Lipkowitz, K. B.; Raghothama, S.; Yang, J. *Am. Chem. Soc.* **1992**, 114, 1554–1562.
31. Konishi, K.; Yahara, K.; Toshishige, H.; Aida, T.; Inoue, S. *J. Am. Chem. Soc.* **1994**, 116, 1337–1344.
32. Asakawa, M.; Brown, C. L.; Pasini, D.; Stoddart, J. F.; Wyatt, P. G. *J. Org. Chem.* **1996**, 61, 7234–7235.
33. Chen, H.; Ogo, S.; Fish, R. H. *J. Am. Chem. Soc.* **1996**, 118, 4993–5001.
34. Zhang, X. X.; Bradshaw, J. S.; Izatt, R. M. *Chem. Rev.* **1997**, 97, 3313–3361.
35. Gavin, J. A.; García, M. E.; Benesi, A. J.; Mallouk, T. E. *J. Org. Chem.* **1998**, 63, 7663–7669.
36. Liu, Y.; You, C. C.; Wada, T.; Inoue, Y. *J. Org. Chem.* **1999**, 64, 3630–3634.
37. Rekharsky, M.; Inoue, Y. *J. Am. Chem. Soc.* **2000**, 122, 4418–4435.
38. Ramírez, J.; Ahn, S.; Grigorean, G.; Lebrilla, C. B. *J. Am. Chem. Soc.* **2000**, 122, 6884–6890.
39. Stevenson, C. D.; Cashion, D. K. *J. Org. Chem.* **2000**, 65, 7588–7594.
40. Titration of compound **2a** was not successful above its CAC because the concentrations required were too large for the UV–Vis experimental conditions.
41. Scatchard plots showed no aggregation induced cooperativity upon binding of compound **2b** by the dyes showing a straight line for host–guest ratios till 1:1. Larger excess of host leads to a non linear plot probably due to a change in the stoichiometry of the complexes formed.
42. Sussman, J. L.; Harel, M.; Frolow, F.; Oefner, C.; Goldman, A.; Toker, L.; Silman, L. *Science* **1991**, 253, 872–879.
43. Ma, J. C.; Dougherty, D. A. *Chem. Rev.* **1997**, 97, 1303–1324.
44. In a similar way as described for amino acids compound **2b** should exist as bis-zwitterionic species at neutral or slightly acidic pH.
45. Since we have not found any aggregation induced binding cooperativity we assume for the modelling studies a single host–guest complex.
46. McDonald, D. Q.; Still, W. C. *J. Am. Chem. Soc.* **1996**, 118, 2073–2077.
47. Lipkowitz, K. B.; Pearl, G.; Coner, B.; Peterson, M. A. *J. Am. Chem. Soc.* **1997**, 119, 600–610.
48. Kolossváry, L. *J. Am. Chem. Soc.* **1997**, 119, 10233–10234.
49. Lipkowitz, K. B.; Coner, R.; Peterson, M. A.; Morreale, A.; Shakelford, J. *J. Org. Chem.* **1998**, 63, 732–745.
50. Lipkowitz, K. B. *Acc. Chem. Res.* **2000**, 33, 555–562.
51. Sijbesma, R. P.; Nolte, R. J. M. *J. Org. Chem.* **1991**, 56, 3122–3124.
52. Connors, K. A. *Binding Constants*. Wiley: New York, 1987.
53. Schneider, H.-J.; Yatsimirsky, A. *Principles and Methods in Supramolecular Chemistry*; Wiley: Chichester, 2000.
54. Mohamadi, F.; Richards, N. G. J.; Guida, W. C.; Liskamp, R.; Caufield, C.; Chang, G.; Hendrickson, T.; Still, W. C. *J. Comput. Chem.* **1990**, 11, 440.
55. Still, W. C.; Tempczyk, A.; Hawley, R. C.; Hendrickson, T. *J. Am. Chem. Soc.* **1990**, 61, 4439–4449.